 CMES, vol.91, no.6, pp.445-461, 2013

Mixed-mode Fracture Mechanics Analysis of Large-scale Cracked Structures Using Partitioned Iterative Coupling Method

Yasunori Yusa[1] **and Shinobu Yoshimura**[1]

Abstract: For large-scale fracture mechanics simulation, a partitioned iterative coupling method is investigated. In this method, an analysis model is decomposed into two domains, which are analyzed separately. A crack is introduced in one small domain, whereas the other large domain is a simple elastic body. Problems concerning fracture mechanics can be treated only in the small domain. In order to satisfy both geometric compatibility and equilibrium on the domain boundary, the two domains are analyzed repeatedly using an iterative solution technique. A benchmark analysis was performed in order to validate the method and evaluate its computational performance. The computed stress intensity factors were as accurate as those obtained using the conventional method and the theoretical solution, and the computational performance was comparable. Based on a benchmark, a cracked structural component model having three million degrees of freedom was analyzed. Mode-I, mode-II, and mode-III stress intensity factors were successfully obtained after several iteration steps.

Keywords: Computational fracture mechanics, finite element method, stress intensity factor, three-dimensional, iterative method.

1 Introduction

Large-scale computational fracture mechanics is required in order to analyze cracked structures in the real world. Several practical studies were performed in order to analyze a real three-dimensional structure with a crack [Ural, Heber, Wawrzynek, Ingraffea, Lewicki, and Neto (2005); Schöllmann, Fulland, and Richard (2003); Diamantoudis and Labeas (2005); Richard, Sander, Fulland, and Kullmer (2008); Barlow and Chandra (2005)]. For an uncracked structure, massively parallel finite element analyses (FEA) were performed on supercomputers or personal computer (PC) clusters [Ogino, Shioya, Kawai, and Yoshimura (2005); Bhardwaj, Pierson,

[1] The University of Tokyo, Tokyo, Japan

Reese, Walsh, Day, Alvin, Peery, Farhat, and Lesoinne (2002)]. Various approaches have been proposed for analyzing large-scale three-dimensional fracture problems. Some problems associated with these approaches were under a mixed-mode stress state. Ural, Heber, Wawrzynek, Ingraffea, Lewicki, and Neto (2005) used both a finite element method (FEM) and a boundary element method (BEM), and their solvers were run on a PC cluster. A crack was introduced on a complex-shaped free surface and a crack propagation problem was analyzed. Schöllmann, Fulland, and Richard (2003) used a sub-modeling approach, which is also referred to as a global–local zooming method. In their study, stress analysis of a global model was first conducted using tetrahedral finite elements, and the analysis results were then mapped into a small sub-model with hexahedral finite elements. Stress intensity factors (SIFs) and crack propagation criteria are evaluated using the sub-model. The global model was then remeshed with the propagated crack shape. Diamantoudis and Labeas (2005) also used the zooming method to analyze a structure with mode-I semi-elliptical cracks. Since the global model used in their study contained no cracks, cracks were introduced in the local domains of several parts. In the zooming method, the one-way mapping means that either geometric compatibility or equilibrium cannot be satisfied between the two domains. Richard, Sander, Fulland, and Kullmer (2008) used the FEM, and Barlow and Chandra (2005) adopted the BEM. They analyzed structural components with a propagation problem of surface ellipse-like cracks. Kamaya, Miyokawa, and Kikuchi (2010) used s-version FEM (SFEM) [Fish (1992)] for a problem of interacting surface cracks. In the SFEM, the global model and the local model (the sub-model) are connected by Lagrange multipliers, and the two models are solved monolithically. Lagrange multipliers are known to increase the condition number, which is the maximum eigenvalue divided by the minimum eigenvalue of a generated stiffness matrix. In conjugate gradient (CG) method, which is frequently used for large-scale FEA, a large condition number degrades its convergence property. Sukumar, Chopp, and Moran (2003) adopted extended FEM (XFEM) [Moës, Dolbow, and Belytschko (1999)] for a three-dimensional crack propagation problem. In the XFEM, a Heaviside function representing a crack is superposed on finite element interpolation functions. An uncracked mesh with a crack function is solved monolithically, and thus XFEM modeling also causes ill-conditioned stiffness matrix, which is not friendly to large-scale analyses. The finite element alternating method (FEAM) [Nishioka and Atluri (1983)] uses a theoretical solution and FEM for a crack and for an uncracked global model, respectively, which are solved alternately. The FEAM was afterward extended to SGBEM–FEM alternating method for a non-planar crack and mixed-mode non-planar crack propagation using BEM, instead of using the theoretical solution [Nikishkov, Park, and Atluri (2001); Han and Atluri (2002)]. In the SGBEM–FEM, a global uncracked FEM mesh and a local cracked SGBEM

mesh are solved alternately to satisfy equilibrium using forces on a mesh boundary and forces on a crack surface. Several three-dimensional numerical experiments using the SGBEM–FEM and using the XFEM showed that the SGBEM–FEM can allow a much more coarse global mesh to obtain accurate stress intensity factors than the XFEM [Dong and Atluri (2013)]. Tetrahedral-element-based virtual crack closure-integral methods (VCCMs) [Okada and Kamibeppu (2005); Okada, Kawai, and Araki (2008)], which are SIF evaluation methods, were proposed for large-scale three-dimensional computational fracture mechanics. Tetrahedral elements are more popular in large-scale FEA than hexahedral elements because automatic mesh generation techniques can be used.

There are a number of problems that must be addressed with regard to large-scale FEA with fracture mechanics. The first problem is related to mesh generation. It is difficult to generate a three-dimensional mesh that represents a complex shape that is also adapted to a crack tip singularity. The second problem is nonlinearity. Several nonlinear phenomena, such as plasticity, creep, large strain, contact, and friction, tend to occur near cracks, whereas the field far from the crack remains linear-elastic or has weak nonlinearity. In order to address these problems, we adopted a partitioned iterative coupling method, which was imported from the field of fluid–structure interaction coupling [Matthies and Steindorf (2003); Yamada and Yoshimura (2008); Minami and Yoshimura (2010)]. In the method, an analysis model is decomposed into a domain near a crack tip (a local domain: Ω^L) and a domain far from the crack (a global domain: Ω^G) as in Fig. 1. Troublesome issues concerning fracture mechanics can only be treated on the local domain. The two domains are analyzed separately with assumed boundary conditions of $\mathbf{u}_\Gamma$ and $\mathbf{f}_\Gamma$ on the domain boundary Γ. In order to satisfy the geometric compatibility and equilibrium on the domain boundary, these domains are analyzed repeatedly with the assumed boundary conditions successively updated using an iterative solution technique. A converged solution that satisfies both compatibility and equilibrium can finally be obtained.

In the present paper, the partitioned iterative coupling method is described in the next section, and several mixed-mode fracture mechanics analyses using the methodology are presented. In the analysis, stress intensity factors were evaluated only on a local mesh, whereas a global mesh was a simple elastic body without a crack. A benchmark problem was analyzed in order to validate the proposed method and compare the proposed method with the conventional FEM. A cracked structural component model with a quarter-circular corner crack was analyzed. Conclusions are finally given after the numerical experiments.

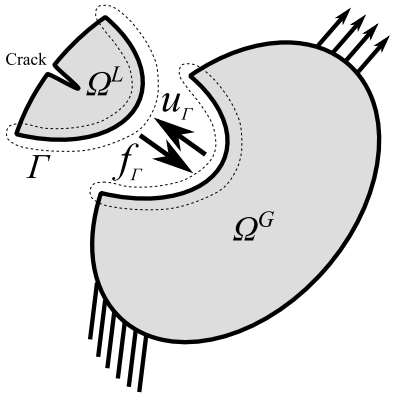

Figure 1: Decomposed analysis model and assumed boundary conditions on the domain boundary.

2 Methods

2.1 Model Decomposition

An analysis model is decomposed into two domains, as shown in Fig. 1. In the present study, decomposition patterns are determined using the following strategies.

1. A crack must be introduced in the local domain.
2. The size and scale of the local domain should be small.
3. On each domain, the volume of finite elements should not vary widely because wide distribution of the volume increases the condition number of the stiffness matrix.

2.2 Partitioned Coupling

Since the two domains are analyzed separately in partitioned coupling methods, geometric compatibility and equilibrium on the domain boundary are not satisfied in general. However, in the partitioned iterative coupling method, they become satisfied by using an iterative solution technique. A local analysis is represented as

$$\mathbf{f}_\Gamma^{(k+1)} = -K_L\left(\mathbf{u}_\Gamma^{(k)}\right) \tag{1}$$

and a global analysis is represented as

$$\mathbf{u}_\Gamma^{(k+1)} = K_G\left(\mathbf{f}_\Gamma^{(k+1)}\right) \tag{2}$$

where k is an iteration step, $\mathbf{u}_\Gamma$ is a displacement vector on the domain boundary Γ, $\mathbf{f}_\Gamma$ is a force vector on Γ, K_L is a function in which a local analysis is performed with enforced displacement boundary conditions $\mathbf{u}_\Gamma$ on Γ that returns a reaction force vector $-\mathbf{f}_\Gamma$, and K_G is also a function in which a global analysis is performed with external force boundary conditions $\mathbf{f}_\Gamma$ on Γ that returns $\mathbf{u}_\Gamma$. Note that the sign of the external force is opposite that of the reaction force. From Eqs. 1 and 2,

$$\mathbf{u}_\Gamma^{(k+1)} = K_G\left(-K_L\left(\mathbf{u}_\Gamma^{(k)}\right)\right) \tag{3}$$

can be obtained. A residual vector $\mathbf{r}$ is defined as

$$\mathbf{r}^{(k+1)} = \mathbf{u}_\Gamma^{(k)} - \mathbf{u}_\Gamma^{(k+1)} = \mathbf{u}_\Gamma^{(k)} - K_G\left(-K_L\left(\mathbf{u}_\Gamma^{(k)}\right)\right). \tag{4}$$

If geometric compatibility on the domain boundary is satisfied, the residual vector should become

$$\mathbf{r}^{(k+1)} = \mathbf{0}. \tag{5}$$

This is the equation to be solved using the iterative algorithm described in the next subsection. In addition, based on Eqs. 1, 4, and 5, that equilibrium also becomes satisfied as

$$\begin{aligned}
&\mathbf{f}_\Gamma^{(k+1)} - \mathbf{f}_\Gamma^{(k+2)} \\
&= -K_L\left(\mathbf{u}_\Gamma^{(k)}\right) + K_L\left(\mathbf{u}_\Gamma^{(k+1)}\right) \\
&= -K_L\left(\mathbf{u}_\Gamma^{(k+1)} + \mathbf{r}^{(k+1)}\right) + K_L\left(\mathbf{u}_\Gamma^{(k+1)}\right) = \mathbf{0}.
\end{aligned} \tag{6}$$

2.3 Iterative Solution Algorithm

In the partitioned iterative coupling method, the two domains are solved using an iterative solution technique. The Block Gauss–Seidel method, line extrapolation method, Newton method, or Broyden method is frequently used to solve fluid–structure interaction coupling problems [Matthies and Steindorf (2003); Yamada and Yoshimura (2008); Minami and Yoshimura (2010)]. In the present study, as a solid–solid interaction coupling problem, the block Gauss–Seidel method with Aitken relaxation is used to solve Eq. 5. The Block Gauss–Seidel method is a fixed-point iteration method, in which one domain is first solved with assumed external force boundary conditions on the domain boundary, and displacements on the domain boundary are obtained. The other domain is then solved with enforced displacement boundary conditions of the obtained displacements, and reaction forces are obtained. The obtained reaction forces are used for new assumed external force

boundary conditions at the next iteration step. These processes are repeated, and a converged solution is finally obtained. Both compatibility and equilibrium would be satisfied by the converged solution. In order to avoid a rigid-body mode of a local model, a local model is determined to be analyzed with assumed enforced displacement boundary conditions on the domain boundary, while a global model is analyzed using assumed external displacement boundary conditions.

In order to stabilize and accelerate the convergence of block Gauss–Seidel iteration, the Aitken extrapolation method [Minami and Yoshimura (2010)] is used for relaxation. When displacements $\mathbf{u}_\Gamma$ on the domain boundary are mapped from one domain to another domain, $\mathbf{u}_\Gamma$ is relaxed by a relaxation parameter ω as follows:

$$\mathbf{u}_\Gamma^{(k+1)} = \mathbf{u}_\Gamma^{(k)} - \omega\left(\mathbf{u}_\Gamma^{(k)} - \tilde{\mathbf{u}}_\Gamma^{(k+1)}\right). \tag{7}$$

Note that k is an iteration step and $\tilde{\mathbf{u}}_\Gamma$ is a displacement vector on the domain boundary before the relaxation. The relaxation parameter is calculated at every iteration step using the Aitken extrapolation method as

$$\omega^{(k+1)} = -\omega^{(k)} \frac{\mathbf{r}^{(k)^{\mathrm{T}}}\left(\mathbf{r}^{(k+1)} - \mathbf{r}^{(k)}\right)}{||\mathbf{r}^{(k+1)} - \mathbf{r}^{(k)}||^2} \tag{8}$$

where $\mathbf{r}_\Gamma$ is a residual vector. The Aitken method is based on one-dimensional quasi-Newton method.

The algorithm of the block Gauss–Seidel method with Aitken relaxation is summarized in the following pseudo code.

$k \leftarrow 0$; $\tau \leftarrow 10^{-3}$; $\omega^{(0)} \leftarrow 0.1$
$\mathbf{f}_\Gamma^{(0)} \leftarrow \mathbf{0}$; $\mathbf{u}_\Gamma^{(0)} \leftarrow \mathbf{0}$; $\tilde{\mathbf{u}}_\Gamma^{(0)} \leftarrow K_G\left(\mathbf{f}_\Gamma^{(0)}\right)$; $\mathbf{r}^{(0)} \leftarrow -\tilde{\mathbf{u}}_\Gamma^{(0)}$
while $||\mathbf{r}^{(k)}||/||\mathbf{r}^{(0)}|| > \tau$ **do**
  $\mathbf{f}_\Gamma^{(k+1)} \leftarrow -K_L\left(\mathbf{u}_\Gamma^{(k)}\right)$
  $\tilde{\mathbf{u}}_\Gamma^{(k+1)} \leftarrow K_G\left(\mathbf{f}_\Gamma^{(k+1)}\right)$
  $\mathbf{r}^{(k+1)} \leftarrow \mathbf{u}_\Gamma^{(k)} - \tilde{\mathbf{u}}_\Gamma^{(k+1)}$
  $\omega^{(k+1)} \leftarrow -\omega^{(k)} \frac{\mathbf{r}^{(k)^{\mathrm{T}}}\left(\mathbf{r}^{(k+1)} - \mathbf{r}^{(k)}\right)}{||\mathbf{r}^{(k+1)} - \mathbf{r}^{(k)}||^2}$
  $\mathbf{u}_\Gamma^{(k+1)} \leftarrow \mathbf{u}_\Gamma^{(k)} - \omega^{(k+1)}\mathbf{r}^{(k+1)}$
  $k \leftarrow k+1$
end while

In the algorithm, K_G is a function of input assumed external force boundary conditions $\mathbf{f}_\Gamma$ and output displacements $\tilde{\mathbf{u}}_\Gamma$. Here, K_L is also a function of input assumed enforced displacement boundary conditions $\mathbf{u}_\Gamma$ and output reaction forces $-\mathbf{f}_\Gamma$. Fi-

nally, τ is a tolerance parameter. In the present study, the tolerance τ and the initial relaxation factor $\omega^{(0)}$ are always set to 10^{-3} and 0.1, respectively.

3 Results and Discussion

3.1 Analysis of the Benchmark Model

A benchmark problem involving a 45-deg oblique circular crack embedded in an infinite body subjected to uniform tension was analyzed in order to validate our solver and to compare the proposed method with a conventional FEM solver. The infinite body was modeled as a finite cube, as shown in Fig. 2. Its mesh is shown in Fig. 3, which was visualized using ADVENTURE AutoGL [Kawai (2006)]. For symmetry, the mesh is a half model, and its finite elements are isoparametric quadratic tetrahedral elements. A crack, whose surface is shown on the right, is introduced to the local mesh. The numbers of elements, nodes, and degrees of freedom (DOFs) are, respectively, 6,796, 10,845, and 32,535 for the global mesh, and are, respectively, 57,056, 79,579, and 238,737 for the local mesh. The numbers of nodes and DOFs are 617 and 1,851, respectively, for the domain boundary. Although the local mesh is larger in scale than the global mesh in such a simple benchmark model, the local mesh becomes much smaller in the real model described in the next subsection.

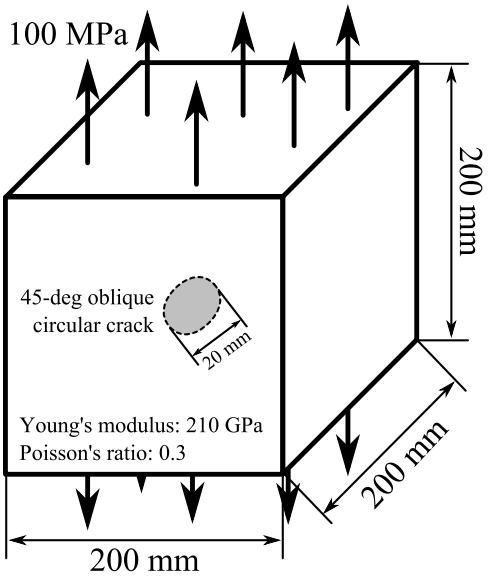

Figure 2: A 45-deg oblique circular crack embedded in a finite cube.

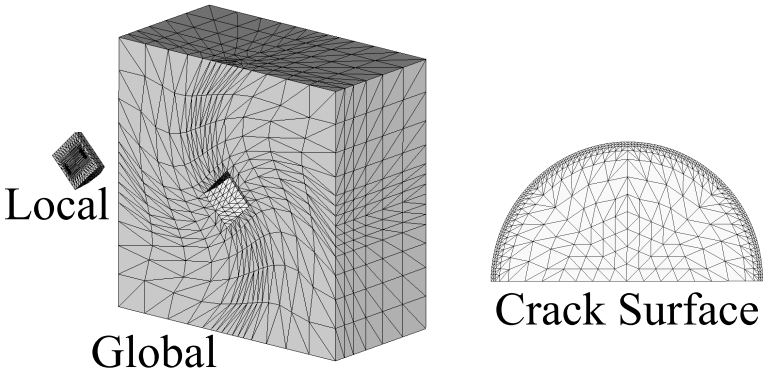

Figure 3: A decomposed half-model mesh for the benchmark analysis and its crack surface mesh.

Mode-I, mode-II, and mode-III stress intensity factors were computed using a virtual crack closure-integral method based on quadratic tetrahedral elements [Okada, Kawai, and Araki (2008)]. Figure 4 shows the computed SIFs of the proposed method, the conventional FEM, and the theoretical solution. The horizontal axis represents a normalized angle $2\phi/\pi$ of crack front coordinates, while the vertical axis represents normalized SIFs F_{I}, F_{II} and F_{III}. The theoretical solution is a superposition of an embedded circular crack in an infinite body subjected to pure tension and subjected to pure shearing. The former solution was introduced by Irwin in 1962, and the latter solution was introduced by Kassir and Sih in 1966 [Murakami, Aoki, Hasebe, Itoh, Miyata, Miyazaki, Terada, Tohgo, Toya, and Yuuki (1987)]. The theoretical solution for normalized stress intensity factors is as follows:

$$F_{\mathrm{I}} = \frac{K_{\mathrm{I}}}{\sigma_0\sqrt{\pi a}} = \frac{2}{\pi}, \tag{9}$$

$$F_{\mathrm{II}} = \frac{K_{\mathrm{II}}}{\tau_0\sqrt{\pi a}} = \frac{4\sin\phi}{(2-\nu)\pi} \tag{10}$$

and

$$F_{\mathrm{III}} = \frac{K_{\mathrm{III}}}{\tau_0\sqrt{\pi a}} = \frac{4(1-\nu)\cos\phi}{(2-\nu)\pi}. \tag{11}$$

K_{I}, K_{II}, and K_{III} are mode-I, mode-II, and mode-III SIFs, respectively. $\sigma_0 = 50$ MPa is tensile loading, and $\tau_0 = 50$ MPa is shear loading. π is a circular constant, $a =$ 10 mm is the crack radius, ϕ is the angle of the crack front coordinates, and $\nu = 0.3$

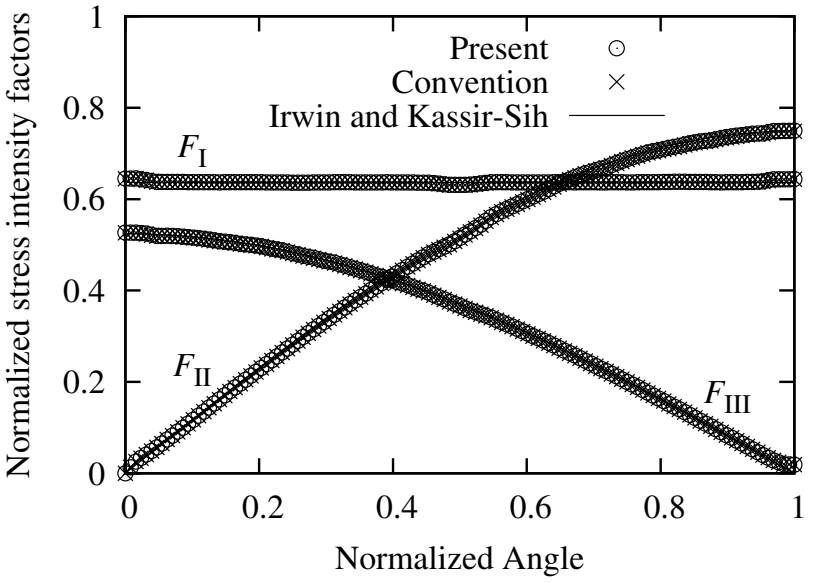

Figure 4: Computed stress intensity factors of the benchmark analysis.

is Poisson's ratio. In Fig. 4, the numerical solutions obtained by the proposed method and the conventional FEM are in very good agreement and are also in good agreement with the theoretical solution.

Figure 5 shows the convergence history of the partitioned iterative coupling algorithm. The horizontal axis represents the iteration count k, and the vertical axis represents the relative residual 2-norm $||\mathbf{r}^{(k)}||/||\mathbf{r}^{(0)}||$. A converged solution was successfully obtained after eight iteration steps. Using the PC described in Tab. 1, the computation time and memory usage were measured, and the results are presented in Tab. 2. Intel Math Kernel Library PARDISO, which is a direct linear system solver, was used for matrix factorization (Cholesky LDL factorization) and triangular solution (forward and backward substitutions). The partitioned iterative coupling solver required 36 s to solve the benchmark, whereas the conventional FEM solver required 35 s. In the proposed method, since the coupling iteration frequently calls the phase of triangular solution, the proposed method requires more computation time than the conventional method. However, in general, matrix factorization dominates the computation time because of its high-order computational complexity. The solver of the present study is not as slow as the conventional FEM solver. On the other hand, the measured memory usage was comparable for the two

solvers.

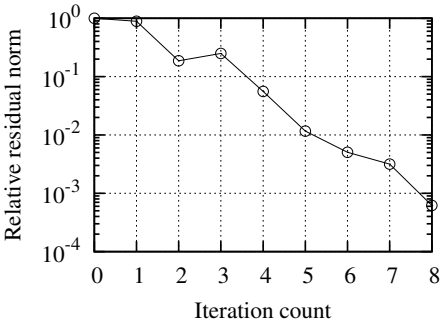

Figure 5: Convergence history of the benchmark analysis.

Table 1: Specifications of the personal computer used in the present study.

CPU	Intel Core i7-3930K (Sandy Bridge)
RAM	DDR3 SDRAM PC3-12800, 64 GB
OS	Debian GNU/Linux 6.0 (squeeze)
Compiler	Intel C Compiler 12.1
	Intel Math Kernel Library 10.2

Table 2: Measured computation time and memory usage of the benchmark analysis.

	Present	Convention
Measured Computation Time		
Total Elapsed Time	36 s	35 s
Matrix Generation	1 s + 7 s	8 s
Matrix Factorization	2 s + 18 s	23 s
Triangular Solution	5 s	$\approx$ 0 s
Other Processes	3 s	4 s
Measured Memory Usage		
Total Memory Usage	2.2 GB	2.3 GB

3.2 Analysis of a Structural Component Model with a Quarter-circular Corner Crack

A structural component model of a curved pipe with a nozzle in which a quarter-circular corner crack is introduced was analyzed using the partitioned iterative coupling method. The model is shown in Fig. 6, and its mesh is shown in Fig. 7. In Fig. 7, the left-hand and center images in the figure represent both show a global mesh and a local mesh. The crack surface mesh is magnified and shown on the right. The numbers of elements, nodes, and DOFs of the global mesh are 758,656, 1,079,880, and 3,239,640, respectively, and the numbers of elements, nodes, and DOFs of the local mesh are 23,960, 34,865 and 104,595, respectively. The ratio of the global number of DOFs to the local number of DOFs is 31:1, which means that the local mesh is much smaller in size and scale than the global mesh. The stress analysis results are shown in Fig. 8. The deformation is magnified by a factor of 10, and the color contour represents von Mises' equivalent stress.

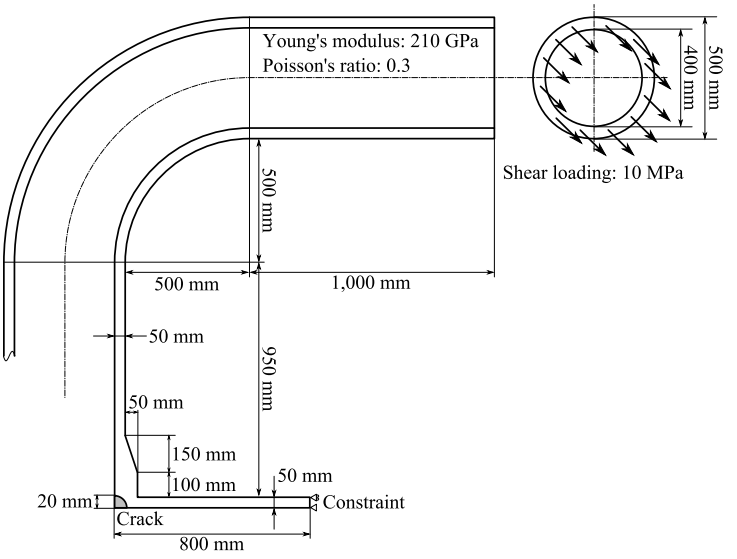

Figure 6: A curved pipe with a nozzle in which a quarter-circular corner crack is introduced.

Stress intensity factors of K_{I}, K_{II} and K_{III} were evaluated on the local mesh using the stress analysis results. The computed SIFs are shown in Fig. 9. The horizontal axis represents a normalized angle of quarter-circular crack coordinates, whereas the vertical axis represents the computed SIFs.

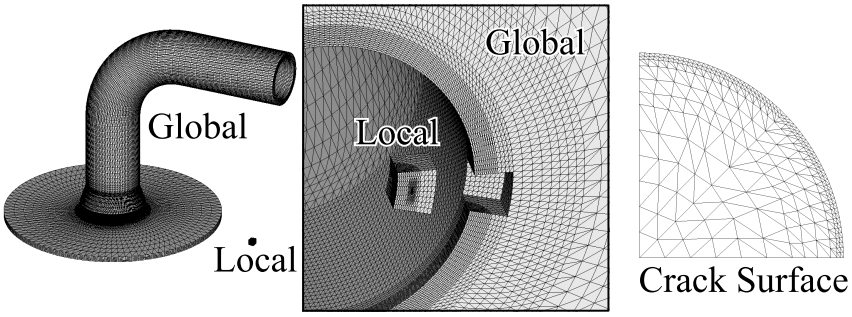

Figure 7: Two views of a decomposed mesh for the structural component analysis and its crack surface mesh.

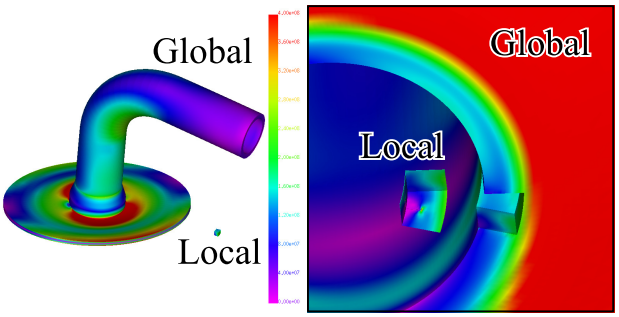

Figure 8: A stress analysis result of the structural component analysis. Its deformation is magnified by 10, and its color contour represents von Mises' equivalent stress, the unit of which is Pa.

The computational performance was measured using a PC (see Tab. 1). Figure 10 shows the convergence history. The horizontal axis shows the iteration count, and the vertical axis shows the relative residual norm. A converged solution was obtained after eight iterations. The total computation time was 1,440 s, where matrix factorization on the global mesh required 1,182 s. The details of the computation time and memory usage are listed in Tab. 3. In the present study, a direct linear solver of Intel Math Kernel Library PARDISO was used for a problem involving three million DOFs. However, for more than tens of millions of DOFs, direct linear solvers become useless because of the long computation time and excessive memory usage. Iterative solvers based on the conjugate gradient method are commonly used for large-scale parallel FEA [Ogino, Shioya, Kawai, and Yoshimura (2005); Bhardwaj, Pierson, Reese, Walsh, Day, Alvin, Peery, Farhat, and Lesoinne

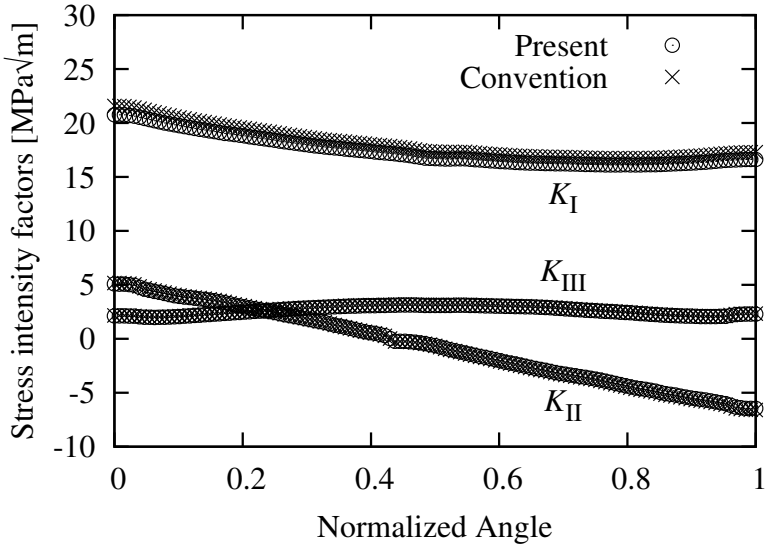

Figure 9: Computed stress intensity factors of the structural component analysis.

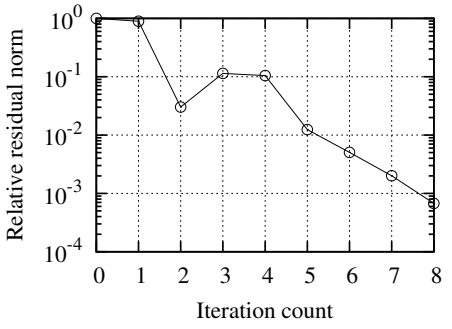

Figure 10: A convergence history of the structural component analysis.

(2002)]. In the CG method, the convergence property is strongly influenced by the condition number of the stiffness matrix. Since the condition number is increased by a large difference of element volume, the element volume distribution was investigated, as shown in Fig. 11. In the histogram, the horizontal axis shows the element volume, and the vertical axis shows the normalized frequency. The maximum and minimum values of the global mesh are 1.23×10^{-5} m^3 and 4.63×10^{-9}

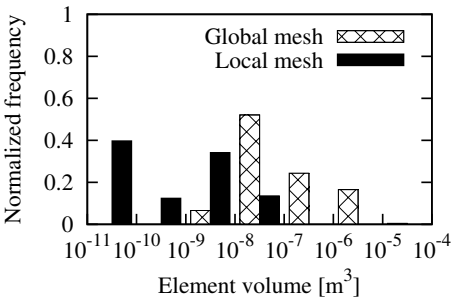

Figure 11: Element volume distribution of the structural component model mesh. The maximum and minimum values of the global mesh are 1.23×10^{-5} m^3 and 4.63×10^{-9} m^3, respectively. The maximum and minimum values of the local mesh are 6.66×10^{-8} m^3 and 1.94×10^{-11} m^3, respectively.

Table 3: Measured computation time and memory usage of the structural component analysis.

	Present	Convention
Measured Computation Time		
Total Elapsed Time	1,440 s	1,414 s
Matrix Generation	89 s + 3 s	96 s
Matrix Factorization	1,182 s + 4 s	1,268 s
Triangular Solution	126 s	16 s
Other Processes	36 s	34 s
Measured Memory Usage		
Total Memory Usage	55.2 GB	56.5 GB

m^3, respectively, and the maximum and minimum values of the local mesh are 6.66×10^{-8} m^3 and 1.94×10^{-11} m^3, respectively. If a conventional FEM solver was selected, the ratio of the maximum volume to the minimum volume would be $(1.23 \times 10^{-5}\ \text{m}^3)/(1.94 \times 10^{-11}\ \text{m}^3) = 6.34 \times 10^5$. On the other hand, in the case of the proposed method, the volume ratio becomes $(1.23 \times 10^{-5}\ \text{m}^3)/(4.63 \times 10^{-9}\ \text{m}^3) = 2.66 \times 10^3$ and $(6.66 \times 10^{-8}\ \text{m}^3)/(1.94 \times 10^{-11}\ \text{m}^3) = 3.43 \times 10^3$. The volume ratio digit is reduced to two thirds in the mesh. For larger-scale problems than the mesh, the volume ratio digit remains constant or sometimes becomes

larger. This is because the maximum element volume value of the global mesh may become large according to its mesh patterns, whereas other values remain approximately constant. In addition, the shape, size, and scale of the local model would be approximately the same for any problem.

4 Conclusions

In the present study, three-dimensional mixed-mode stress intensity factor analyses were performed using the partitioned iterative coupling method. In this method, an analysis model is decomposed into two domains, which are analyzed separately and repeatedly using an iterative solution technique. The stress intensity factors are evaluated on one small domain, while the other large domain becomes an uncracked elastic body. A benchmark problem of a 45-deg oblique circular crack embedded in a finite cube was analyzed. In the benchmark analysis, the computed SIFs were as accurate as those computed using the conventional method and the theoretical solution. The number of iteration steps and the computation time were measured in order to compare the proposed method with the conventional FEM. The computation time was comparable for the two methods. A structural component model of a curved pipe with a nozzle, in which a quarter-circular corner crack is introduced, was then analyzed. Mixed-mode SIFs were successfully computed using a model having three million degrees of freedom.

In the future, a crack propagation problem and a nonlinear fracture problem, like the mixed-mode problem investigated herein, are important problems for real cracked structures and must be investigated using the partitioned iterative coupling method. In such problems, problems concerning fracture mechanics would also occur only in the local domain. In addition, the global mesh and the local mesh are conforming at the domain boundary in the present study. The proposed method can be extended for nonconforming meshing with carefully interpolating nodal reaction forces.

Acknowledgement: The present study was supported by a MEXT grant as part of *HPCI Strategic Program Field No. 4: Next-generation Industrial Innovations*. The authors would also like to thank the members of the ADVENTURE project for engaging in helpful discussions.

References

Barlow, K. W.; Chandra, R. (2005): Fatigue crack propagation simulation in an aircraft engine fan blade attachment. *International Journal of Fatigue*, vol. 27, pp. 1,661–1,668.

Bhardwaj, M.; Pierson, K.; Reese, G.; Walsh, T.; Day, D.; Alvin, K.; Peery, J.; Farhat, C.; Lesoinne, M. (2002): Salinas: a scalable software for high-performance structural and solid mechanics simulations. In *Proceedings of the ACM/IEEE Supercomputing Conference 2002*, pp. 1–19.

Diamantoudis, A. T.; Labeas, G. N. (2005): Stress intensity factors of semi-elliptical surface cracks in pressure vessels by global–local finite element methodology. *Engineering Fracture Mechanics*, vol. 72, pp. 1,299–1,312.

Dong, L.; Atluri, S. N. (2013): Fracture & fatigue analyses: SGBEM–FEM or XFEM? part 2: 3D solids. *Computer Modeling in Engineering and Sciences*, vol. 90, no. 5, pp. 379–413.

Fish, J. (1992): The s-version of the finite element method. *Computers and Structures*, vol. 43, no. 3, pp. 539–547.

Han, Z. D.; Atluri, S. N. (2002): SGBEM (for cracked local subdomain)–FEM (for uncracked global structure) alternating method for analyzing 3D surface cracks and their fatigue-growth. *Computer Modeling in Engineering and Sciences*, vol. 3, no. 6, pp. 699–716.

Kamaya, M.; Miyokawa, E.; Kikuchi, M. (2010): Growth prediction of two interacting surface cracks of dissimilar sizes. *Engineering Fracture Mechanics*, vol. 77, no. 16, pp. 4,466–4,485.

Kawai, H. (2006): ADVENTURE AutoGL: a handy graphics and GUI library for researchers and developers of numerical simulations. *Computer Modeling in Engineering and Sciences*, vol. 11, no. 3, pp. 111–120.

Matthies, H.; Steindorf, J. (2003): Partitioned strong coupling algorithms for fluid–structure interaction. *Computers and Structures*, vol. 81, pp. 805–812.

Minami, S.; Yoshimura, S. (2010): Performance evaluation of nonlinear algorithms with line-search for partitioned coupling techniques for fluid–structure interactions. *International Journal for Numerical Methods in Fluids*, vol. 64, no. 10–12, pp. 1,129–1,147.

Moës, N.; Dolbow, J.; Belytschko, T. (1999): A finite element method for crack growth without remeshing. *International Journal for Numerical Methods in Engineering*, vol. 46, pp. 131–150.

Murakami, Y.; Aoki, S.; Hasebe, H.; Itoh, Y.; Miyata, H.; Miyazaki, N.; Terada, H.; Tohgo, K.; Toya, M.; Yuuki, R. (1987): *Stress Intensity Factor Handbook*. Pergamon Press.

Nikishkov, G. P.; Park, J. H.; Atluri, S. N. (2001): SGBEM–FEM alternating method for analyzing 3D non-planar cracks and their growth in structural components. *Computer Modeling in Engineering and Sciences*, vol. 2, no. 3, pp. 401–422.

Nishioka, T.; Atluri, S. N. (1983): Analytical solution for embedded elliptical cracks, and finite element alternating method for elliptical surface cracks, subjected to arbitrary loadings. *Engineering Fracture Mechanics*, vol. 17, no. 3, pp. 247–268.

Ogino, M.; Shioya, R.; Kawai, H.; Yoshimura, S. (2005): Seismic response analysis of nuclear pressure vessel model with ADVENTURE system on the Earth Simulator. *Journal of the Earth Simulator*, vol. 2, pp. 41–54.

Okada, H.; Kamibeppu, T. (2005): A virtual crack closure-integral method (VCCM) for three-dimensional crack problems using linear tetrahedral finite elements. *Computer Modeling in Engineering and Sciences*, vol. 10, no. 3, pp. 229–238.

Okada, H.; Kawai, H.; Araki, K. (2008): A virtual crack closure-integral method (VCCM) to compute the energy release rates and stress intensity factors based on quadratic tetrahedral finite elements. *Engineering Fracture Mechanics*, vol. 75, no. 15, pp. 4,466–4,485.

Richard, H. A.; Sander, M.; Fulland, M.; Kullmer, G. (2008): Development of fatigue crack growth in real structures. *Engineering Fracture Mechanics*, vol. 75, pp. 331–340.

Schöllmann, M.; Fulland, M.; Richard, H. A. (2003): Development of a new software for adaptive crack growth simulations in 3D structures. *Engineering Fracture Mechanics*, vol. 70, pp. 249–268.

Sukumar, N.; Chopp, D. L.; Moran, B. (2003): Extended finite element method and fast marching method for three-dimensional fatigue crack propagation. *Engineering Fracture Mechanics*, vol. 70, pp. 29–48.

Ural, A.; Heber, G.; Wawrzynek, P. A.; Ingraffea, A. R.; Lewicki, D. G.; Neto, J. B. C. (2005): Three-dimensional, parallel, finite element simulation of fatigue crack growth in a spiral bevel pinion gear. *Engineering Fracture Mechanics*, vol. 72, pp. 1,148–1,170.

Yamada, T.; Yoshimura, S. (2008): Line search partitioned approach for fluid–structure interaction analysis of flapping wing. *Computer Modeling in Engineering and Sciences*, vol. 24, no. 1, pp. 51–60.